New Journal of Physics
The open-access journal for physics

Matchgate quantum computing and non-local process analysis

S Ramelow[1,2,4,5], **A Fedrizzi**[1,4,5], **A M Steinberg**[1,3] **and A G White**[1]

[1] Centre for Quantum Computer Technology and Department of Physics, University of Queensland, QLD 4072, Australia
[2] Faculty of Physics, University of Vienna, Boltzmanngasse 5, 1090 Vienna, Austria
[3] Center for Quantum Information and Quantum Control, Institute for Optical Sciences, Department of Physics, University of Toronto, 60 St. George Street, Toronto, ON, M5S 1A7, Canada
E-mail: sven.ramelow@univie.ac.at and a.fedrizzi@uq.edu.au

New Journal of Physics **12** (2010) 083027 (10pp)
Received 23 March 2010
Published 11 August 2010
Online at http://www.njp.org/
doi:10.1088/1367-2630/12/8/083027

Abstract. In the circuit model, quantum computers rely on the availability of a universal quantum gate set. A particularly intriguing example is a set of two-qubit-only gates: 'matchgates', along with SWAP (the exchange of two qubits). In this paper, we show a simple decomposition of arbitrary matchgates into better-known elementary gates and implement a matchgate in a single-photon linear optics experiment. The gate performance is fully characterized via quantum process tomography. Moreover, we represent the resulting reconstructed quantum process in a novel way, as a fidelity map in the space of all possible non-local two-qubit unitaries. We propose the *non-local distance*—which is independent of local imperfections such as uncorrelated noise or uncompensated local rotations—as a new diagnostic process measure for the non-local properties of the implemented gate.

In quantum computation, an essential requirement of the circuit model is a universal gate set, which enables the approximation of any given unitary process to arbitrary precision [1]. The advantages and disadvantages of various gate sets are still being actively explored; for example, one set may be more natural than others for interpreting a certain problem or, in a given physical

[4] These authors contributed equally to this work.
[5] Authors to whom any correspondence should be addressed.

architecture, one set may require far less resources than another. The best known gate-set class is that of any entangling 2-qubit gate in combination with arbitrary single-qubit unitaries [2]: most famously the 2-qubit CNOT gate in conjunction with the 1-qubit Hadamard, H, and phase, T, gates. Circuits constructed solely of the CNOT and H gates can be simulated efficiently with a classical computer [1]. However, the addition of the T gate—itself also efficiently simulatable—enables universal quantum computing (which of course is generally believed to be *not* efficiently simulatable). Another important gate-set class uses 3-qubit entanglers, such as the Toffoli gate—which has only recently been demonstrated in linear optics [3] and ion traps [4]—along with H.

In this paper, we demonstrate a new gate-set class based *only* on 2-qubit gates, specifically the *matchgate* [5], which can be entangling, and the SWAP gate, which is strictly non-entangling [6, 7]. Matchgates—originally introduced in graph theory [5]—are 2-qubit unitaries,

$$\mathrm{G_{AB}} = \begin{pmatrix} a_{11} & 0 & 0 & a_{12} \\ 0 & b_{11} & b_{12} & 0 \\ 0 & b_{21} & b_{22} & 0 \\ a_{21} & 0 & 0 & a_{22} \end{pmatrix}, \tag{1}$$

where the 1-qubit unitaries

$$\mathrm{A} = \begin{pmatrix} a_{11} & a_{12} \\ a_{21} & a_{22} \end{pmatrix} \quad \text{and} \quad \mathrm{B} = \begin{pmatrix} b_{11} & b_{12} \\ b_{21} & b_{22} \end{pmatrix} \tag{2}$$

are members of $U(2)$ with $\det(\mathrm{A}) = \det(\mathrm{B})$ and act on the even and the odd 2-qubit parity subspaces, respectively. Note that the determinant condition precludes gates such as SWAP, which otherwise could be constructed as $\mathrm{G_{IX}} = \mathrm{SWAP}$, where I is the 1-qubit identity. Matchgates include a rich number of entangling gates—including maximal entangling gates—as well as many classes of local gates. If matchgates act only between nearest-neighbor qubits, then the resulting circuit can be efficiently simulated classically [5]. In this context, matchgates relate to systems of non-interacting fermions [6]. Moreover, they are connected to one-dimensional (1D) quantum Ising models: explicit matchgate circuits for simulation of such strongly correlated quantum systems have been constructed in [8]. However, if matchgates are also allowed to operate between *next*-nearest neighbors—a seemingly trivial change achieved via SWAP gates—then the circuit can perform universal quantum computation [7]. Clearly, the resulting universal gate set is entirely different from the two mentioned above.

Here we show how to realize arbitrary matchgates using circuit elements already demonstrated in a range of physical architectures; we go on to demonstrate and measure matchgate operation in a linear optics photonic system, quantifying their performance with a new method for experimental analysis of two-qubit gates.

Figure 1(a) shows the decomposition of an arbitrary matchgate, $\mathrm{G_{AB}}$, into CNOT ($\mathrm{CNOT} = |0\rangle\langle 0| \otimes \mathrm{I} + |1\rangle\langle 1| \otimes \mathrm{X}$), controlled-unitary and single-qubit gates. Recall that, depending on the parity of the input state into the matchgate, either A or B acts on the two qubits. The first step of our general decomposition is to encode the parity of the two-qubit state onto one of the qubits. The first CNOT gate turns the bottom qubit into state $|0\rangle$ for even-parity inputs ($|00\rangle \to |00\rangle$ and $|11\rangle \to |10\rangle$) and into $|1\rangle$ for odd-parity inputs ($|01\rangle \to |01\rangle$ and $|10\rangle \to |11\rangle$). This qubit then

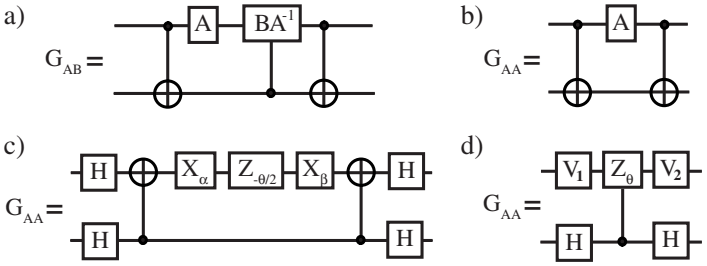

Figure 1. (a) Decomposition of general matchgates G_{AB}. (b) Simplified decomposition of symmetric matchgates G_{AA}, as described in the text. (c) The same gate after flipping the CNOTs with H's and decomposing HAH into X- and Z-rotations. (d) Further simplification shows that G_{AA}, up to a global phase, can be implemented using a single CZ_θ and local unitaries $V_1 = HX_\alpha$ and $V_2 = Z_{-\theta/2}X_\beta H$, where α, β and θ are related to A via $HAH = X_\alpha Z_{-\theta/2} X_\beta$. For G_{HH}, $\theta = \pi$, and $CZ_\theta \rightarrow CZ$.

acts as the control for the controlled unitary, CU (CU $= |0\rangle\langle 0| \otimes \mathrm{I} + |1\rangle\langle 1| \otimes \mathrm{U}$), where $\mathrm{U} = \mathrm{BA}^{-1}$. If the bottom qubit is in state $|0\rangle$ (parity $= 0$), A will act on the top qubit; if it is in state $|1\rangle$ (parity $= 1$), CU will undo A before it performs B. The final CNOT gate returns the qubits from the parity encoding to the original basis.

Note that, alternatively, any 2-qubit operation could be implemented with three CNOT gates and eight-single-qubit unitaries [9], or with two '$\mathcal{B}$'-gates (yet to be experimentally demonstrated) and six single-qubit unitaries [10]. Our decomposition, which offers a starting point for further simplifications, in contrast, requires fewer gates and allows one to recast matchgate circuits (e.g. those in [8]) into circuits consisting of more familiar quantum gates—the CNOT [11, 12], the more general CU [3] and single-qubit rotations, all of which have been individually implemented in various architectures.

We now show how to build the matchgates required for a universal gate set. The universality proof in [7] relies on showing how matchgates and SWAP can be applied to implement another universal set: H, T and CZ. As outlined in the appendix, each logical qubit has to be encoded in two (or four) physical qubits. The required matchgate set is then G_{XX}, G_{TT} and G_{HH}. These gates are all symmetric, i.e. A = B, and the circuit of figure 1(a) is greatly simplified, because $\mathrm{A}^{-1}\mathrm{A} = \mathrm{I}$: the controlled unitary turns into a 'controlled identity'. The resulting circuit diagram, shown in figure 1(b), still requires two 2-qubit gates. It does, however, resemble the general construction of a CU [13] gate, i.e. it can be replaced by a single CU and four single-qubit unitaries in the following way: we flip the CNOT(s) upside down by adding four Hadamards—$\overline{\mathrm{CNOT}} \equiv (\mathrm{H}\otimes\mathrm{H}) \times \mathrm{CNOT} \times (\mathrm{H}\otimes\mathrm{H})$—and rewrite the resulting central unitary HAH, up to a global phase, as $X_\alpha Z_{-\theta/2} X_\beta$ [13] (figure 1(c)). The rotations X_α and X_β commute with their respective CNOT(s), which allows us to express the two-qubit part of the operation as a single controlled CZ_θ (figure 1(d)). This simplified circuit for G_{AA} can now be directly implemented in bosonic systems using the technique of shortcuts through higher-dimensional Hilbert spaces [3].

Turning back to the universal matchgate set, we find that $G_{XX} = \mathrm{X} \otimes \mathrm{X}$ and $G_{TT} = \mathrm{T} \otimes \mathrm{I}$—both operations are local and can be done trivially in a photonic architecture with waveplates or interferometers. Similarly, SWAP is a straightforward procedure in optics, either in free-space or

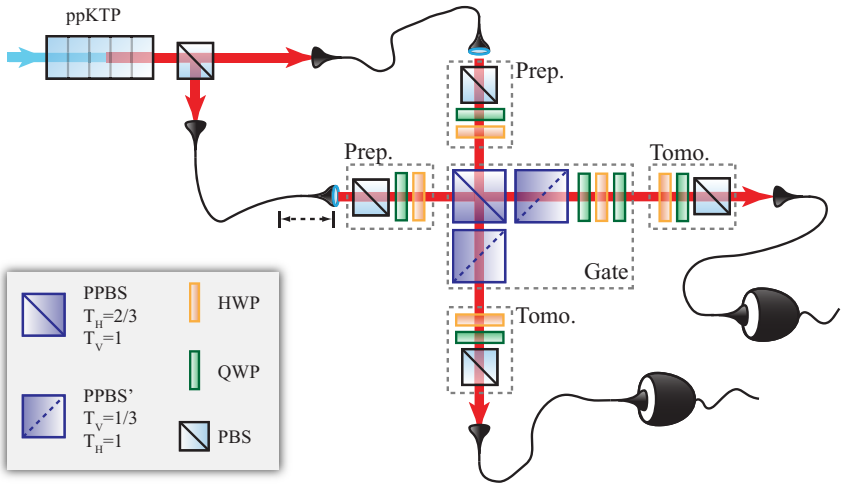

Figure 2. Experimental scheme. Orthogonally polarized photon pairs are created in a nonlinear ppKTP crystal that is pumped by a 410 nm laser diode, using focusing parameters from [17]. The photons are split at a polarizing beamsplitter (PBS), collected and guided to the circuit with single-mode optical fibers. The input states are prepared with a PBS, one quarter- and one half-wave plate (QWP, HWP) (Prep.). The photons are then superposed on a partially polarizing beamsplitter (PPBS), which transmits 2/3 of horizontal, $|H\rangle$, and perfectly reflects vertical, $|V\rangle$, light. Loss elements (PPBS′) correct the respective amplitudes and the unknown phase shift at the central PPBS is compensated by an combination of a QWP, an HWP and another QWP in one output port of the PPBS. If compensated correctly, only the input term $|HH\rangle$ picks up a phase shift of π due to non-classical interference, which realizes a bit-flipped CZ when measured in coincidence. The photons are then jointly analyzed with a QWP, an HWP and a PBS (Tomo.) before they are detected by two single-photon detectors. The rotations for the four single-qubit unitaries required for G_{HH} in figure 1(d) are incorporated into the preparation and measurement waveplate settings.

integrated circuits. The one non-trivial gate to be demonstrated is

$$G_{HH} = \frac{1}{\sqrt{2}} \begin{pmatrix} 1 & 0 & 0 & 1 \\ 0 & 1 & 1 & 0 \\ 0 & 1 & -1 & 0 \\ 1 & 0 & 0 & -1 \end{pmatrix}, \tag{3}$$

which is a non-local, maximally entangling gate. For this gate the decomposition yields $\theta = \pi$ and therefore CZ_θ in figure 1(d) is the well-known CZ gate. Experimentally, we can therefore implement G_{HH} using polarization-encoded single photons, partially polarizing beam splitters and coincidence detection [14]–[16]. The experimental setup is described in figure 2.

We characterized our gate using full quantum *process* tomography [18], preparing 16 combinations of the states $\{|H\rangle, |V\rangle, |D\rangle = 1/\sqrt{2}(|H\rangle + |V\rangle), |R\rangle = 1/\sqrt{2}(|H\rangle + \mathrm{i}|V\rangle)\}$ at each input and projecting into an overcomplete set of 36 measurements at the outputs. The

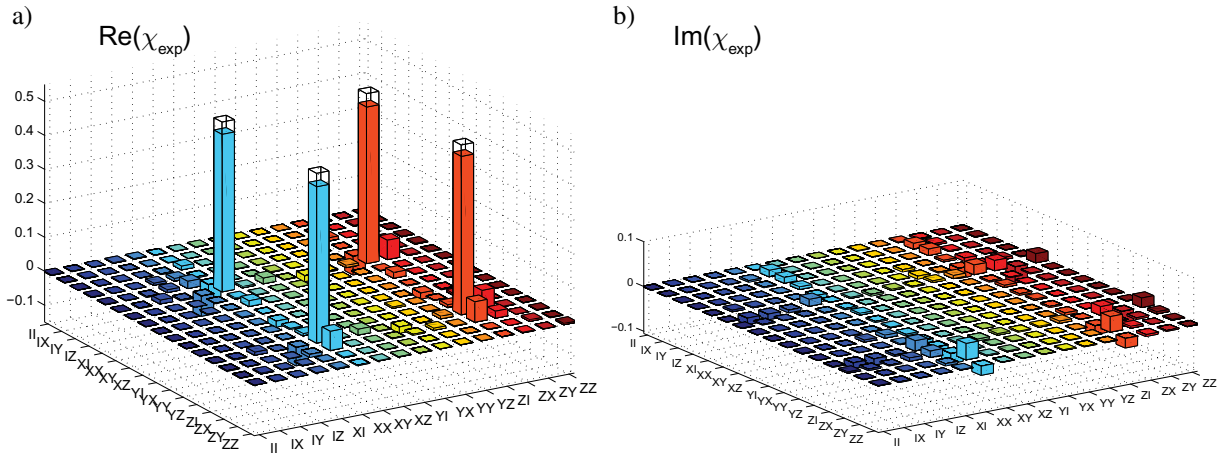

Figure 3. (a) Real and (b) imaginary parts of the G_{HH} process matrix χ_{exp} reconstructed from quantum process tomography measurements. The wire frames represent the ideal process χ_{ideal}. The process fidelity of χ_{exp} with χ_{ideal} was $92.3 \pm 0.2\%$. We did not apply any numeric local rotations to optimize this result in contrast to e.g. [3].

photons were then detected in coincidence. The resulting process matrix χ_{exp}, reconstructed via maximum-likelihood estimation, is shown in figure 3. The process fidelity [22] with χ_{ideal} is $92.3 \pm 0.2\%$, where the error was calculated assuming Poissonian count statistics. We attribute the remaining errors to non-ideal waveplates, imperfections in the spatial and temporal mode-overlap, as well as in the splitting ratios of the PPBSs.

The question remains—how well have we actually implemented a matchgate? A single process fidelity, such as that calculated above, reveals the overlap between the experimental process and the corresponding, ideal target process. However, it does not yield any information about the way in which the process is not ideal—is it just mixed due to random noise or are we in fact implementing a different unitary process than we actually thought? In particular, we are interested in the *non-local* properties of the quantum process, as they define its entangling power and errors in them cannot be corrected with local operations.

Interestingly, as shown in [19], out of the 15 real parameters that define a unitary 2-qubit operator $U \in \mathrm{SU}(4)$, only three actually describe the nonlocal part of the unitary, the remaining 12 relating to local transformations:

$$U = (u_1 \otimes v_1) \mathrm{e}^{-\mathrm{i}/2(c_1\sigma_x\otimes\sigma_x + c_2\sigma_y\otimes\sigma_y + c_3\sigma_z\otimes\sigma_z)} (u_2 \otimes v_2). \tag{4}$$

This decomposition allows a very intuitive geometrical representation of local equivalence classes. The three non-local parameters c_1, c_2 and c_3 can be used to construct a three-dimensional space of non-local gates. Symmetries reduce this space to a tetrahedron, shown in figure 4(a), the so-called Weyl chamber [20]. Each point in this chamber represents all locally equivalent gates with unique non-local properties (with the exception of the $c_3 = 0$ plane, which is symmetric around the line $[\pi/2, 0, 0] \rightarrow [\pi/2, \pi/2, 0]$); the CNOT and the CZ gate, and therefore also the G_{HH}, are locally equivalent and located at $[\pi/2, 0, 0]$. Using a method from [20], one can directly check whether two gates are locally equivalent, which confirms the results obtained from our matchgate decomposition in figure 1.

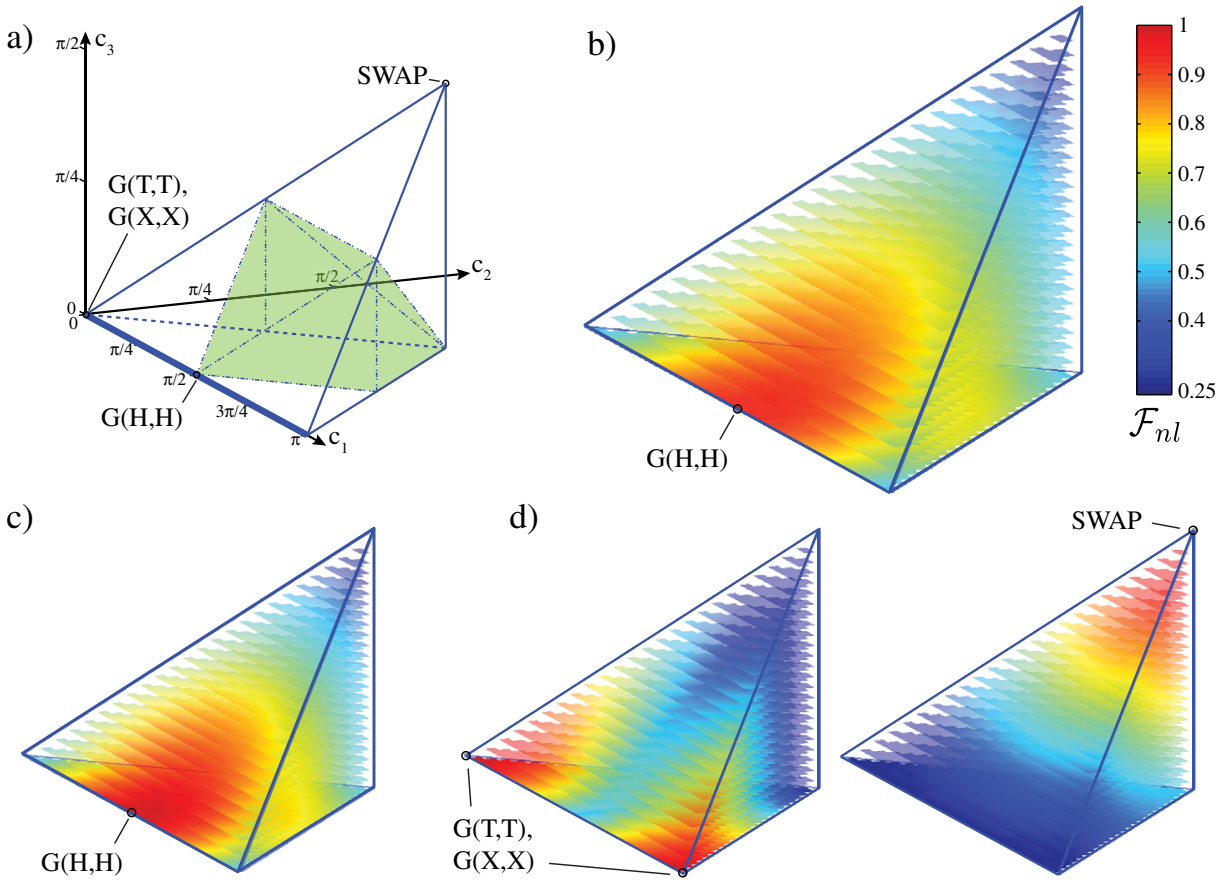

Figure 4. (a) Tetrahedron depicting the space of all non-local two-qubit unitary gates. All local gates $u \otimes v$, such as G_{XX} and G_{TT}, are represented by [0,0,0]; SWAP is located at $[0, \pi/2, \pi/2]$. The shaded volume represents the space of all perfect entanglers [20], i.e. gates that can turn separable states into Bell states. The (thick blue) line $[\gamma, 0, 0]$ contains all G_{AA} gates, which are equivalent to CU [3]. G_{HH} is located at its midpoint $[\pi/2, 0, 0]$ and is therefore the only symmetric matchgate that is maximally entangling. (b) Fidelity map for the experimentally reconstructed G_{HH} process matrix showing the fidelity (equation (5)) with respect to 6201 evenly spread ideal 2-qubit operators and optimizing over all local unitary degrees of freedom. The maximum fidelity is $94.7 \pm 0.3\%$ at $\sim[\pi/2, 0, 0]$, which is exactly the point representing G_{HH}. (c–d) Theoretical fidelity maps for several ideal gates: the target gate G_{HH} and the local gates G_{XX} and G_{TT} as well as SWAP.

In order to illustrate our experimental process in the Weyl chamber and to find the non-local unitary gate closest to it, we numerically translated 6201 evenly spaced ideal 2-qubit operators defined by (4) into their process representation and then calculated their maximal *non-local* process fidelity,

$$\mathcal{F}_{\mathrm{nl}}(c_1, c_2, c_3) = \max_{u_1 \ldots v_2} \mathcal{F}(\chi_{\mathrm{exp}}, \chi(c_1 \ldots c_3, u_1 \ldots v_2)), \tag{5}$$

to χ_{exp} by numerical optimization over the local transformations u_1, v_1 and u_2, v_2. Applying numeric local rotations to optimize a process fidelity to a specific (ideal) target process is

common practice in linear optics quantum experiments, see e.g. [3, 14, 21]. This is motivated by the high precision and ease with which local unitaries can be implemented in optics. We extend this by calculating the non-local fidelity for every point in the Weyl chamber. The result is a three-dimensional process fidelity map, shown in figure 4(b). After optimization over the local unitaries, we find a maximum process fidelity for our experimental gate of $94.7 \pm 0.3\%$ (increased from 92.3%, figure 3) at $[c_1, c_2, c_3] \sim [\pi/2, 0, 0]$.

For comparison, we show the fidelity maps for the ideal G_{HH} in figure 4(c). The maximum fidelity is, as expected, 1 at $[\pi/2, 0, 0]$. The fidelity of G_{HH} is 50% with local gates and 25% with SWAP, which reflects the fact that the distance in the Weyl chamber to the latter is maximal ($\mathcal{F}$ has a range of $\mathcal{F} \in [0.25, 1]$). The volume of non-local gates with $\geqslant 90\%$ fidelity to χ_{ideal} is 11.6%. For χ_{exp} this volume shrinks to 4.85%, due to decoherence. Ideal fidelity maps for the remaining gates from the universal matchgate set, G_{XX}, G_{TT} and SWAP in figure 4(d) complete the picture.

We can now define a new process distance measure—the *non-local distance*, $\Delta_{nl} \equiv \sqrt{\Delta c_1^2 + \Delta c_2^2 + \Delta c_2^2}$, where $\Delta_{nl} \in [0, \pi]$ and Δc_i is the difference between the coordinates of a target unitary gate and the coordinates for the maximum fidelity for a given process $\mathcal{F}_{nl}(c_1, c_2, c_3)_{max}$ obtained from the optimization, equation (5). This distance can of course also be used for two ideal unitaries in the chamber. According to [22], Δ_{nl} meets all distance measure criteria for pure processes and can be seen as a *diagnostic measure*. To illustrate this, let us compare the process purity to $\mathcal{F}_{nl}$: because it is maximized to an underlying, unitary 2-qubit operation, stripped of its local rotations, it will signal—similar to the purity—when an implemented process is pure. However, in contrast to the purity, $\mathcal{F}_{nl}$ also tells us which operation was in fact implemented.

Our experimental gate is located at a distance $\Delta_{nl} \sim 0$ from the ideal CZ. The implemented gate therefore has—within negligible uncertainties dominated by the numerical optimization—exactly the intended non-local properties. Upon closer inspection, this is a direct consequence of the way the gate is implemented physically. First of all, any uncorrelated noise process, such as depolarization or dephasing [1], acting on the input or output states of our gate is non-unitary and adds mixture to the process, which leads to a uniform decrease of $\mathcal{F}_{nl}$ over the whole non-local space, as illustrated by comparison of the experimental to the ideal fidelity map in figures 4(b) and (c). Secondly, imperfections in optical components such as the PPBS central to our gate equally lead to mixing because the underlying 2-qubit operations for reflectivity values close to $\eta_{ideal} = 1/3$ are non-unitary [23] and do not result in a shift of the gate's position in the unitary space represented by the Weyl chamber. Other imperfections, such as temporal or spatial mode mismatch, can be modeled as incoherent sums of different unitary operations. In this case, fidelity maps would still not show a shift of the non-local location of the resulting process, but rather the emergence of additional local maxima, centered at the non-local positions of the contributing unitary operators. Our optical setup therefore does not have any *non-local, unitary* degrees of freedom in the sense that the available experimental parameters do not allow an actual movement of the fidelity maximum in the Weyl chamber. The physical implementation of the CU gates demonstrated in [3], in contrast, would have allowed a shift of the experimental process along the line marking the symmetric matchgates.

Our non-local process analysis allows us to conclude that the overall quality of our gate implementation cannot be improved by unitary corrections beyond simple local rotations. In other words, apart from local rotations that can be easily applied, the closest unitary gate to the experimentally implemented process is indeed G_{HH}. The remaining reduction in fidelity is

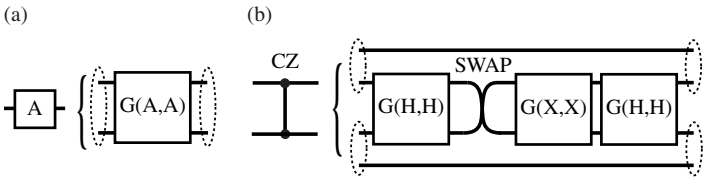

Figure A.1. Matchgate universality proof [7]. (a) Symmetric matchgates G_{AA} act on two physical qubits which represent one logical qubit. (b) CZ can be constructed using symmetric matchgates and SWAP. Dotted ellipses represent logical qubits.

identified as mixture, caused by effects such as higher-order photon emissions from the SPDC source, which is supported by the measured, non-ideal process purity of $89.8 \pm 0.4\%$. Future experimental work will have to focus on removing these noise sources.

In summary, we have implemented a matchgate that allows universal computation when combined with the simple two-qubit SWAP. Our gate decomposition provides a simple procedure to implement known matchgate circuits in linear optics and, vice versa, translate quantum computing algorithms formulated in terms of more common gate sets into physical architectures that are naturally suited for implementing matchgates.

We characterized our gate using quantum process tomography and illustrated the fidelity overlap of the experimental process with all possible non-local gates in the Weyl chamber. We expect this method to develop into a valuable diagnostic tool in quantum information processing, especially in the analysis of noisy processes where it can help identify and distinguish unitary error sources from genuine mixing. Suggested lines for further research in this topic are, for example, how correlated noise influences the non-local properties of a quantum gate and non-local process discrimination [24].

Acknowledgments

We thank B P Lanyon and N K Langford for their valuable input. We acknowledge financial support from the Australian Research Council Discovery and Federation Fellow programs and an IARPA-funded US Army Research Office contract. SR acknowledges financial support from the FWF project CoQuS no. W1210-N16. AMS acknowledges support from the Natural Sciences and Engineering Research Council of Canada, Quantum Works and the Canadian Institute for Advanced Research.

Appendix

We briefly review here the universality proof given by R Jozsa and A Miyake in [7], which involves showing how one can construct an already known universal set from G_{AB} + SWAP. Because G_{AB} is intrinsically a two-qubit gate and does not allow a change of parity of the input state, it is not straightforward to construct arbitrary single-qubit unitaries. This is solved in [7] by encoding the logical qubits $|0\rangle_L$, $|1\rangle_L$ into two physical qubits that have the same parity $|0\rangle_L = |00\rangle$, $|1\rangle_L = |11\rangle$. A symmetric G_{AA} acting on the two physical qubits then performs the single-qubit unitary A on the logical qubit (figure A.1(a)). This 2-qubit encoding is universal

with next-next-nearest neighbor interactions, whereas a more complicated 4-qubit encoding, which requires the nontrivial G_{ZX}, allows universal quantum computing with only next-nearest neigbor interactions [7].

Next, we need an entangling gate that can act between two encoded logical qubits. This can be achieved by adding SWAP, because, as illustrated in figure A.1(b), $CZ = G_{HH} \times SWAP \times G_{XX} \times G_{HH}$, where X denotes the σ_x Pauli operator. In summary, the minimal set of matchgates needed for universal quantum computing is G_{HH} and G_{TT}, which implement the single-qubit gates H and T on the encoded dual-qubit space, and G_{XX}, G_{HH} and SWAP, which together form a CZ.

References

[1] Nielsen M A and Chuang I 2000 *Quantum Computation and Quantum Information* (Cambridge: Cambridge University Press)

[2] Dodd J L, Nielsen M A, Bremner M J and Thew R T 2002 Universal quantum computation and simulation using any entangling Hamiltonian and local unitaries *Phys. Rev.* A **65** 040301

[3] Lanyon B P, Barbieri M, Almeida M P, Jennewein T, Ralph T C, Resch K J, Pryde G J, O'Brien J L, Gilchrist A and White A G 2008 Simplifying quantum logic using higher-dimensional Hilbert spaces *Nat. Phys.* **5** 134–40

[4] Monz T, Kim K, Hänsel W, Riebe M, Villar A S, Schindler P, Chwalla M, Hennrich M and Blatt R 2009 Realization of the quantum Toffoli gate with trapped ions *Phys. Rev. Lett.* **102** 040501

[5] Valiant L G 2002 Quantum circuits that can be simulated classically in polynomial time *SIAM J. Comput.* **31** 1229–54

[6] Terhal B M and DiVincenzo D P 2002 Classical simulation of noninteracting-fermion quantum circuits *Phys. Rev.* A **65** 32325

[7] Jozsa R and Miyake A 2008 Matchgates and classical simulation of quantum circuits *Proc. R. Soc.* A **464** 3089

[8] Verstraete F, Cirac J I and Latorre J I 2009 Quantum circuits for strongly correlated quantum systems *Phys. Rev.* A **79** 032316

[9] Vidal G and Dawson C M 2004 Universal quantum circuit for two-qubit transformations with three controlled-NOT gates *Phys. Rev.* A **69** 010301

[10] Zhang J, Vala J, Sastry S and Whaley K B 2004 Minimum construction of two-qubit quantum operations *Phys. Rev. Lett.* **93** 020502

[11] O'Brien J L, Pryde G J, White A G, Ralph T C and Branning D 2003 Demonstration of an all-optical quantum controlled-NOT gate *Nature* **426** 264–7

[12] Gasparoni S, Pan J W, Walther P, Rudolph T and Zeilinger A 2004 Realization of a photonic controlled-NOT gate sufficient for quantum computation *Phys. Rev. Lett.* **93** 20504

[13] Barenco A, Bennett C H, Cleve R, DiVincenzo D P, Margolus N, Shor P, Sleator T, Smolin J A and Weinfurter H 1995 Elementary gates for quantum computation *Phys. Rev.* A **52** 3457–67

[14] Langford N K, Weinhold T J, Prevedel R, Resch K J, Gilchrist A, O'Brien J L, Pryde G J and White A G 2005 Demonstration of a simple entangling optical gate and its use in Bell-state analysis *Phys. Rev. Lett.* **95** 21

[15] Kiesel N, Schmid C, Weber U, Ursin R and Weinfurter H 2005 Linear optics controlled-phase gate made simple *Phys. Rev. Lett.* **95** 210505

[16] Okamoto R, Hofmann H F, Takeuchi S and Sasaki K 2005 Demonstration of an optical quantum controlled-NOT gate without path interference *Phys. Rev. Lett.* **95** 210506

[17] Fedrizzi A, Herbst T, Poppe A, Jennewein T and Zeilinger A 2007 A wavelength-tunable fiber-coupled source of narrowband entangled photons *Opt. Express* **15** 15377–86

[18] O'Brien J L, Pryde G J, Gilchrist A, James D F V, Langford N K, Ralph T C and White A G 2004 Quantum process tomography of a controlled-NOT gate *Phys. Rev. Lett.* **93** 080502
[19] Kraus B and Cirac J I 2001 Optimal creation of entanglement using a two-qubit gate *Phys. Rev.* A **63** 062309
[20] Zhang J, Vala J, Sastry S and Whaley K B 2003 Geometric theory of nonlocal two-qubit operations *Phys. Rev.* A **67** 042313
[21] Resch K J, O'Brien J L, Weinhold T J, Sanaka K, Lanyon B P, Langford N K and White A G 2007 Entanglement generation by Fock-state filtration *Phys. Rev. Lett.* **98** 203602
[22] Gilchrist A, Langford N K and Nielsen M A 2005 Distance measures to compare real and ideal quantum processes *Phys. Rev.* A **71** 062310
[23] Ralph T C, Langford N K, Bell T B and White A G 2002 Linear optical controlled-NOT gate in the coincidence basis *Phys. Rev.* A **65** 062324
[24] Laing A, Rudolph T and O'Brien J L 2009 Experimental quantum process discrimination *Phys. Rev. Lett.* **102** 160502